CONVECTION IN NORMAL STARS AND METAL-DEFICIENT STARS

K. S. KRISHNA SWAMY*
Goddard Space Flight Center, Greenbelt, Md., U.S.A.

(Received 11 November, 1968)

Abstract. The depths at which convection starts have been calculated for main sequence stars and giant stars of various effective temperatures and hydrogen-to-metal ratios. It is found that for late-type stars of $T_e \gtrsim 4400$ K convection starts at $\tau \gtrsim 0.1$. In metal-deficient stars convection starts at shallower optical depths compared to normal stars of the same spectral type. The larger the metal deficiency, the shallower is the depth at which convection starts. The importance of convection in the study of metal-deficient stars and late type stars are also discussed.

1. Introduction

The outermost layers of a star are in radiative equilibrium regardless of the extent of the inner convective regions. Convection due to overshooting is present in some cases (BÖHM, 1963), but the efficiency of convection is so low that the actual temperature gradient is very close to the radiative temperature gradient. From theoretical considerations, one finds that the atmosphere at great optical depth cannot be in stable radiative equilibrium. Except for very few hot stars the convective zone below the photosphere is present in most of the stars. Recently it has been shown, that convection also plays an important role in metal-deficient stars (KRISHNA SWAMY, 1966a, 1967, 1968a, b; COHEN and STROM, 1968; DENNIS, 1968). It is found that the larger the metal deficiency, the shallower is the depth at which convection starts and, therefore, the greater is the importance of convection.

The mechanical stability of a stellar atmosphere under radiative equilibrium was first studied by SCHWARZSCHILD (1906), who showed that the atmosphere will be convectively unstable if the radiative temperature gradient at any level in a stellar atmosphere exceeds the adiabatic temperature gradient corresponding to the same values of temperature and pressure, i.e.

$$\nabla_{\text{rad}} \equiv \left(\frac{d\ln T}{d\ln P}\right)_{\text{rad}} > \left(\frac{d\ln T}{d\ln P}\right)_{\text{ad}} \equiv \nabla_{\text{ad}} \tag{1}$$

where the subscripts 'rad' and 'ad' denote the radiative and adiabatic temperature gradients, respectively.

UNSÖLD (1930) pointed out that the adiabatic gradient for a gas dissociating into ions and electrons is decreased from the value of a perfect gas. After this work, a large number of investigations have been carried out for different physical conditions (UNSÖLD, 1938; UNDERHILL, 1949; KRISHNA SWAMY, 1961; FISCHEL, 1968). In late-

* National Academy of Sciences-National Research Council, Postdoctoral Research Associate.

Astrophysics and Space Science **3** (1969) 552–563; © *D. Reidel Publishing Company, Dordrecht-Holland*

type stars and in metal-deficient stars the abundance of hydrogen molecule can be quite appreciable (VARDYA, 1966; KRISHNA SWAMY, 1966a, 1967, 1968b). Hence, in these stars convection starts at very shallow optical depths because of the dissociation of the hydrogen molecules. The object of the present paper is to calculate the depth at which convection starts for normal stars and metal-deficient stars of different spectral types. We will also discuss the effect of convection on the observable physical properties of the star.

2. Calculations

Model Atmosphere: The methods and assumptions employed for the model atmosphere calculation are essentially those given by KRISHNA SWAMY (1966a). Here we will briefly mention a few points.

(1) Composition: We take $x=0.75$ and the models are calculated for hydrogen-to-metal ratio (H/M) of 1, 5, 10, 40, and 100 times the solar value. The abundance of the individual elements are fixed using the solar abundances as standard (GOLDBERG *et al.*, 1960).

(2) Opacity: For the calculation of Rosseland mean opacity, we assume the continuous opacity to be due to absorption by H, H^-, H_2^- and H_e^- and scattering by H and H_2.

(3) Equation of state: We consider hydrogen to be in the stages H_2, H_2^+, H^-, H and H^+. Helium is considered only in the neutral state and the metals in neutral and ionized states. Detailed ionization equilibrium of nine elements besides hydrogen is taken into account.

(4) $(T-\tau)$ relation: From an earlier analysis (KRISHNA SWAMY, 1966a, b) it was found that the scaled solar model atmosphere approach was quite adequate for solar-type stars. But for metal-deficient stars, the scaled solar models were not satisfactory. This is due to the fact that the role of convection is far more important in a metal-deficient star than in a normal star of the same spectral type (KRISHNA SWAMY, 1967, 1968a, b). Since we are interested in the depth at which convection starts, we have to know the temperature distribution in the radiative layers of the star. This requires some discussion. As a result of heavy line blanketing, the actual temperature distribution existing in the atmospheres of stars will be modified considerably from the grey body temperature distribution law. Therefore, the line blanketing affects the observable physical properties of a star considerably. So far, only preliminary attempts have been made to calculate the changes in the temperature distribution arising as a result of line blanketing effect in the model atmosphere calculation. However, it is possible to get the temperature distribution of the solar atmosphere from an analysis of the limb darkening observations (MITCHELL, 1959; CAYREL and JUGAKU, 1963). The analytical relation which fits up the temperature distribution obtained from the limb darkening observations is given by (KRISHNA SWAMY, 1966a, 1967),

$$T^4 = \tfrac{3}{4}T_e^4(\tau + 1.39 - 0.815\, e^{-2.54\tau} - 0.025\, e^{-30\tau}). \qquad (2)$$

Here τ is the Rosseland mean optical depth. It has been shown (KRISHNA SWAMY, 1966a, b) that the models based on Equation (2) were also able to reproduce some of the observed profiles of stars of spectral type between K2 and F8. Therefore, for the present study, we have used the analytical temperature distribution given by Equation (2). The use of Equation (2) for the temperature distribution in the radiative zone has the advantage of empirically allowing, to a first approximation, for line blanketing effect.

(5) Surface gravity and effective temperature: We calculated the model atmospheres for various effective temperatures in the range 4000 K to 6000 K. These models were calculated for three values of the surface gravity corresponding to 2×10^4, 2×10^3 and 2×10^2.

(6) Adiabatic Gradient: Since the early start of convection in late-type stars and metal-deficient stars arises primarily as a result of the decrease of the adiabatic gradient brought about as a result of the dissociation of the hydrogen molecule, it is very important to include the effect of hydrogen molecule in addition to others in the calculation of the adiabatic gradient. In the calculation of the adiabatic gradient we have considered all the different species that have been included in the equation of state. The adiabatic gradient is calculated as in VARDYA (1965). For the total internal energy we have included the energy of translation, and the energy due to dissociation and ionization of various hydrogen species and metals.

3. Results of Calculations

The results of the calculations are shown in Figures 1, 5 and 6. It gives a plot of the optical depth at which convection starts as a function of effective temperature for

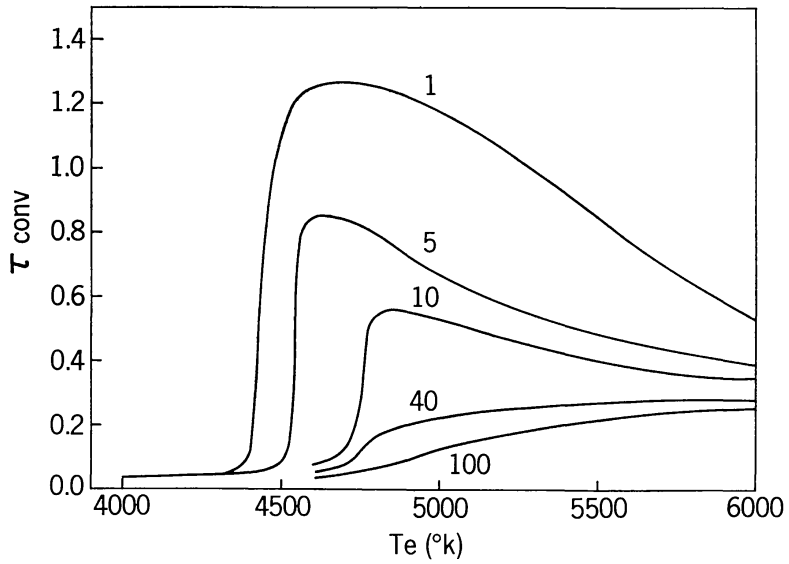

Fig. 1. Optical depth at which convection starts is plotted as a function of effective temperature for $g = 2 \times 10^4$. The number shown at the top of each curve gives the hydrogen-to-metal ratio with respect to that of solar value.

different hydrogen-to-metal ratios. The number shown at the top of each curve gives the hydrogen-to-metal ratio with respect to that of solar value. One can see clearly from Figure 1 that convection starts at shallow optical depths in metal-deficient stars compared to normal stars of the same spectral type. Also convection starts at very shallow optical depths in late-type stars. In fact, calculations extended up to $T_e \sim 3000\,K$ show that curve remains flat throughout this region. It is interesting to note that for models with $(H/M) = 1\,(H/M)_\odot$ the curve falls off steeply for $T_e \gtrsim 4600\,K$. The same trend appears for other cases although they are not as drastic as in the case of $(H/M) = 1\,(H/M)_\odot$. All the curves shown in Figure 1 can be understood in terms of the physical quantities which lead to the inequality of Equation (1). Let us consider the curve corresponding to $(H/M) = 1\,(H/M)_\odot$. The inequality given by Equation (1) can arise because of two reasons. (1) The adiabatic gradient becomes small or (2) the radiative gradient becomes large. The adiabatic gradient becomes small for a gas dissociating into atoms, ions and electrons. The radiative gradient increases when the opacity becomes large. We show in Figure 2 a plot of ∇_{rad} and ∇_{ad} as a function

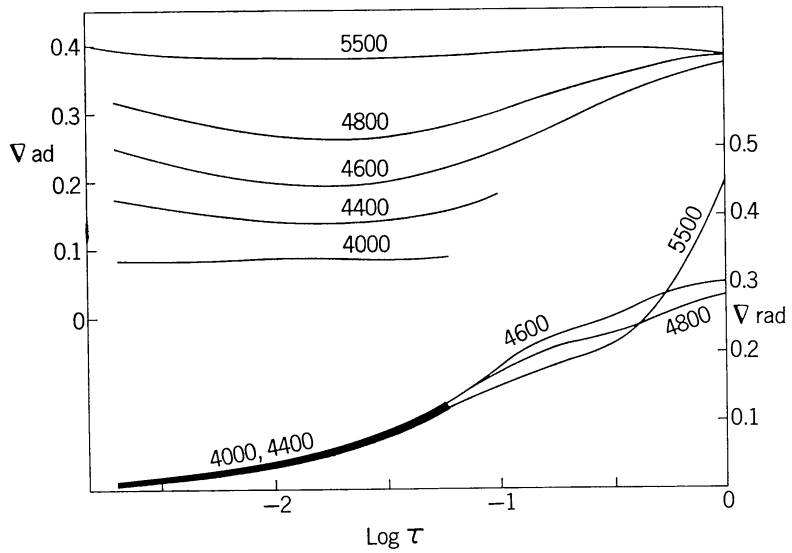

Fig. 2. Radiative gradients and adiabatic gradients are plotted as a function of $\log\tau$ for different effective temperatures. The curves are for $(H/M) = 1\,(H/M)_\odot$ and $g = 2 \times 10^4$.

of $\log\tau$ for different effective temperatures. The dark curve shown in the plot of ∇_{rad} vs. $\log\tau$ is the region where the curves for all the effective temperatures show overlap. One can see clearly that for small effective temperatures the value of the adiabatic gradient decreases considerably from 0.4, the value corresponding to a perfect gas. This arises as a result of the dissociation of the hydrogen molecules which are more abundant in cool stars as can be seen from Table I. However, the value of the radiative gradient does not change drastically with effective temperature. Therefore, the steep fall of the curve in Figure 1 for $T_e \gtrsim 4600\,K$ can be attributed mainly to the decrease in the adiabatic gradient as a result of the dissociation of the hydrogen molecules. For effective temperatures greater than about 5000 K the value

TABLE I

Ratio of the partial pressure of hydrogen molecule to that of hydrogen for $g = 2 \times 10^4$

τ	$A = 1$			$A = 40$		
	T_e (K)			T_e (K)		
	4000	4400	4600	4000	4400	4600
0.01	0.261	0.047	0.020	0.990	0.191	0.085
0.02	0.274	0.051	0.022	1.04	0.207	0.093
0.03	0.269	0.050	0.022	1.03	0.208	0.095
0.05	0.240	0.045	0.020	0.935	0.188	0.087
0.08	0.194	0.037	0.017	0.905	0.156	0.073
0.10	0.169	0.032	0.015	0.700	0.138	0.065
0.20	0.098	0.019	0.009	0.437	0.086	0.041
0.50	0.050	0.009	0.005	0.367	0.039	0.019

of the adiabatic gradient does not change appreciably from the value 0.4. This is due to the fact that in these stars the concentration of hydrogen molecules is small and also the ionization of hydrogen is negligible. But with the increase in effective temperature the radiative gradient increases as a result of the increase in opacity as can be seen from Figure 3. Therefore, the gradual fall of the curve for $T_e \gtrsim 5000\,\mathrm{K}$ is mostly due to the increase in the radiative gradient brought about as a result of the increase in opacity. For cases $(\mathrm{H/M}) > 1\,(\mathrm{H/M})_\odot$, the curves become flatter and flatter compared to normal stars. This is because of the increase in role of molecular hydrogen.

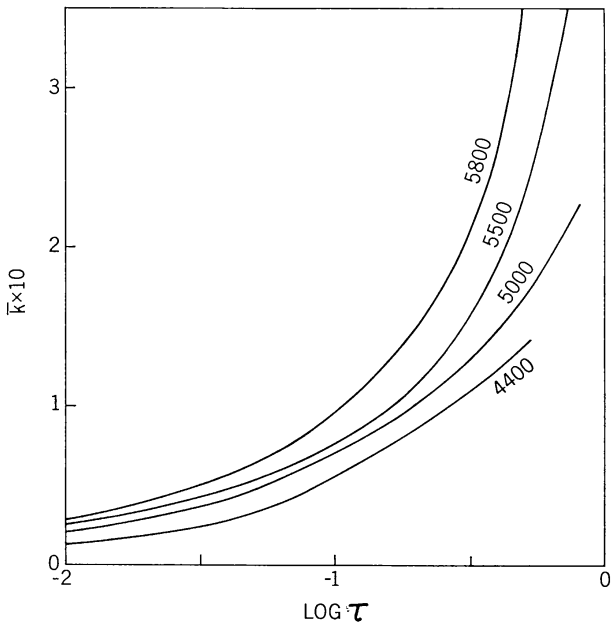

Fig. 3. Rosseland mean opacity is plotted as a function of $\log\tau$ for different effective temperatures. The curves are for $(\mathrm{H/M}) = 1\,(\mathrm{H/M})_\odot$ and $g = 2 \times 10^4$.

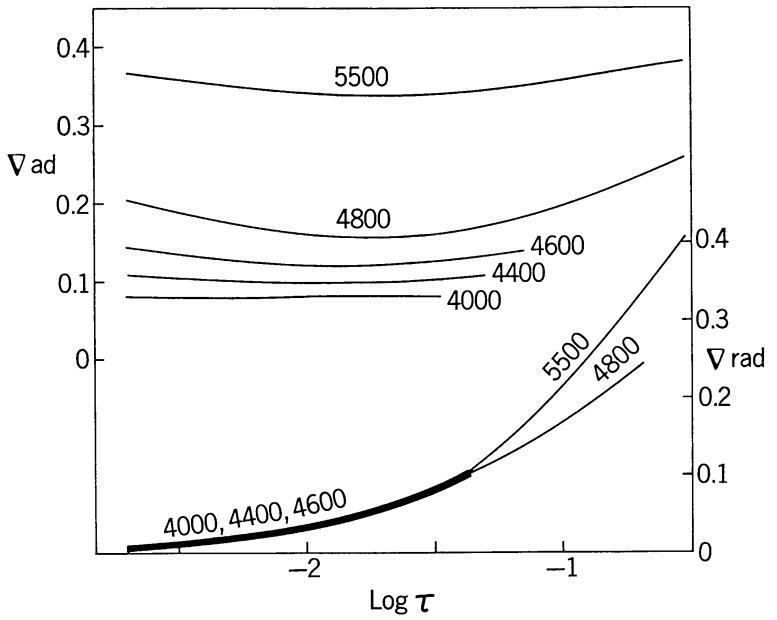

Fig. 4. Same as Figure 2 but for $(H/M) = 40(H/M)_{\odot}$.

As a typical case, we show in Figure 4, a plot of the same physical quantities of Figure 2 for different effective temperatures and for hydrogen-to-metal ratio of 40 times the solar value. For the same physical conditions, we give in Table I, the ratio of the partial pressures of hydrogen molecule to that of hydrogen. One can see from Figure 4 and Table I the important role of hydrogen molecules in metal-deficient stars.

The optical depth at which convection starts for the cases $g = 2 \times 10^3$ and 2×10^2 are shown in Figures 5 and 6. The form of these curves are exactly the same as those of Figure 1. Therefore, all our conclusions as discussed earlier for the case $g = 2 \times 10^4$

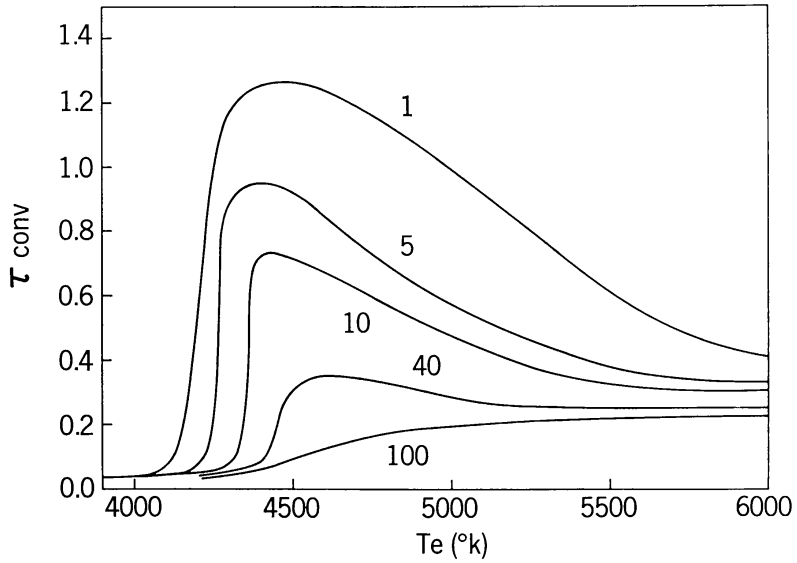

Fig. 5. Same as Figure 1, but for $g = 2 \times 10^3$.

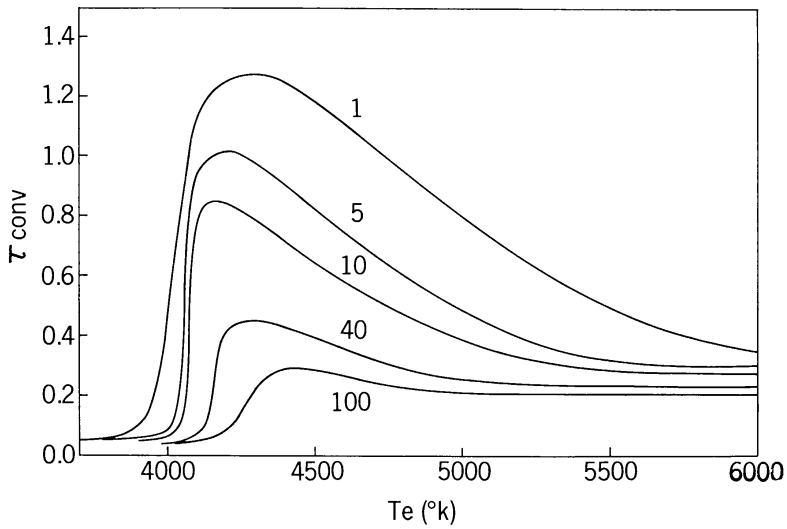

Fig. 6. Same as Figure 1, but for $g = 2 \times 10^2$.

are also valid for the cases $g = 2 \times 10^3$ and 2×10^2. But the importance of hydrogen molecules decreases with the decrease in the surface gravity for the same effective temperature. For this purpose, we show in Figure 7 the optical depth at which convection starts as a function of T_e for the three surface gravities considered and for (H/M) = 1, 10 and 100 times the solar value. One can easily see the shift in the curves with a decrease in surface gravity. The steep fall of the curves move towards lower effective temperatures as the surface gravity is decreased. As pointed out earlier, the steep fall of the curve is essentially due to the dissociation of hydrogen

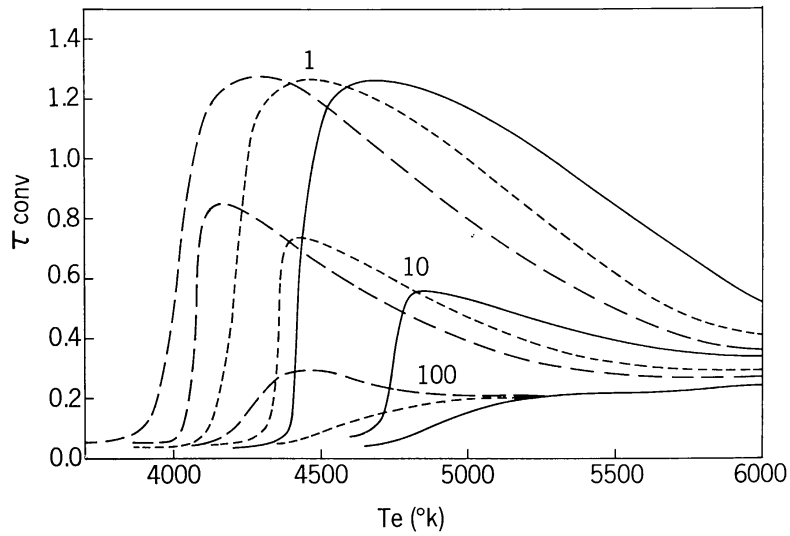

Fig. 7. Optical depth at which convection starts is plotted as a function of effective temperature for three values of hydrogen-to-metal ratios of 1, 10 and 100 times the solar value. Continuous curves, dashed curves and long dashed curves are for $g = 2 \times 10^4$, 2×10^3 and 2×10^2 respectively.

molecule and therefore it depends critically on the abundance of hydrogen molecule. The abundance of hydrogen molecule decreases with an increase in effective temperature or with a decrease in the gravity (Tables II and III). With the result, the reduction in the adiabatic gradient from the perfect gas value is more for the case $g=2\times10^4$ compared to that of $g=2\times10^3$ or 2×10^2 (see Figures 2 and 8). But on the other hand the radiative gradient does not change appreciably with surface gravity. As a result the steep fall of the curve shifts towards smaller effective temperatures with a decrease in the surface gravity.

It is significant to calculate the efficiency of convection as a function of hydrogen-to-metal ratio for different effective temperatures and surface gravities. In Tables IV and V we give the percentage flux carried by convection for the cases $g=2\times10^4$ and 2×10^3. We might mention that the results given in Tables IV and V are based on

TABLE II

Ratio of the partial pressure of hydrogen molecule to that of hydrogen for $g=2\times10^3$

	$A=1$			$A=40$		
τ	T_e (K)			T_e (K)		
	4000	4200	4400	4000	4200	4400
0.01	0.079	0.031	0.012	0.332	0.127	0.051
0.02	0.083	0.032	0.013	0.349	0.136	0.056
0.03	0.081	0.032	0.013	0.342	0.134	0.056
0.05	0.070	0.028	0.012	0.303	0.119	0.050
0.08	0.055	0.022	0.009	0.243	0.096	0.041
0.10	0.047	0.019	0.008	0.211	0.083	0.036
0.20	0.026	0.011	0.005	0.120	0.049	0.022
0.50	0.010	0.005	0.002	0.048	0.021	0.010

TABLE III

Ratio of the partial pressure of hydrogen molecule to that of hydrogen for $g=2\times10^2$

	$A=1$		$A=40$	
τ	T_e (K)		T_e (K)	
	4000	4200	4000	4200
0.01	0.022	0.008	0.092	0.033
0.02	0.023	0.008	0.097	0.036
0.03	0.022	0.009	0.095	0.035
0.05	0.019	0.007	0.082	0.031
0.08	0.015	0.006	0.064	0.025
0.10	0.013	0.005	0.055	0.021
0.20	0.007	0.003	0.030	0.012
0.50	0.003	0.001	0.012	0.005

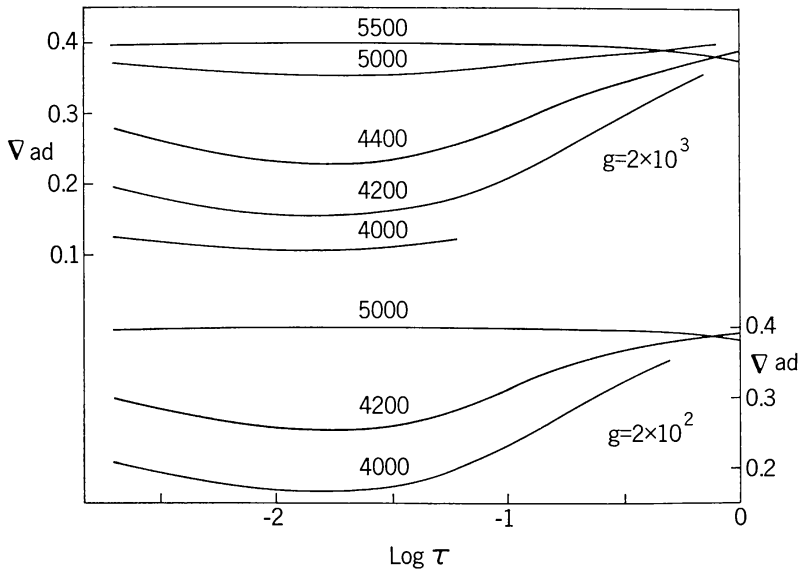

Fig. 8. Adiabatic gradients are plotted as a function of $\log\tau$ for different effective temperatures.

TABLE IV

Percentage flux carried by convection: $g = 2 \times 10^4$

τ \ A	1	5	10	40	100
	$T_e = 4300$ K				
0.5	–	–	2	26	–
1.0	–	–	5	45	–
2.0	–	18	15	62	–
5.0	4	43	57	80	–
10.0	42	70	76	88	–
	$T_e = 4500$ K				
0.5	–	–	–	2	20
1.0	–	–	–	15	43
2.0	–	–	8	43	65
5.0	5	43	56	73	82
10.0	45	69	75	86	88
	$T_e = 5000$ K				
1.0	–	–	–	1	6
2.0	–	–	4	23	38
5.0	5	35	48	63	71
10.0	45	65	71	79	85
	$T_e = 5500$ K				
2.0	–	–	–	2	4
5.0	4	23	32	42	46
10.0	43	58	62	66	69

TABLE V

Percentage flux carried by convection: $g = 2 \times 10^3$

τ \ A	1	5	10	40	100
	$T_e = 4000$ K				
0.5	–	–	–	23	39
1.0	–	–	–	33	57
2.0	–	–	1	45	69
5.0	–	21	41	69	83
10.0	20	63	69	83	93
	$T_e = 4500$ K				
1.0	–	–	–	–	2
2.0	–	–	–	9	30
5.0	–	14	30	58	69
10.0	21	54	62	75	86
	$T_e = 5000$ K				
2.0	–	–	–	1	37
5.0	–	8	17	39	48
10.0	23	51	56	68	71
	$T_e = 5500$ K				
2.0	–	–	–	–	–
5.0	–	3	5	8	10
10.0	23	44	45	48	49

the mixing-length theory of BÖHM-VITENSE (1958). In all the calculations, the ratio of mixing length to pressure scale height is set to be unity. It is interesting to note from the Tables IV and V that in metal-deficient stars, the convective flux carries an appreciable fraction of the total flux. It may also be noted that the efficiency of convection decreases with a decrease in surface gravity.

4. Discussion

As can be seen from Figures 1, 5 and 6, convection starts at shallow optical depths in metal-deficient stars. The larger the metal deficiency, the shallower is the depth at which convection starts. The effect of convection in general is to decrease the actual temperature gradient considerably from the radiative temperature gradient. Therefore, the temperature distribution becomes flat through the atmosphere of the star. Recently we have calculated the temperature distribution of the model atmospheres for different effective temperatures and hydrogen-to-metal ratios. The results of these calculations clearly show the flattening of the temperature distribution with increase in metal deficiency. As a typical case we show in Figure 9 the resultant temperature distributions obtained for $T_e = 5000$ K and for $g = 2 \times 10^4$ and 2×10^3. This has been shown to have an appreciable effect on the observable physical proper-

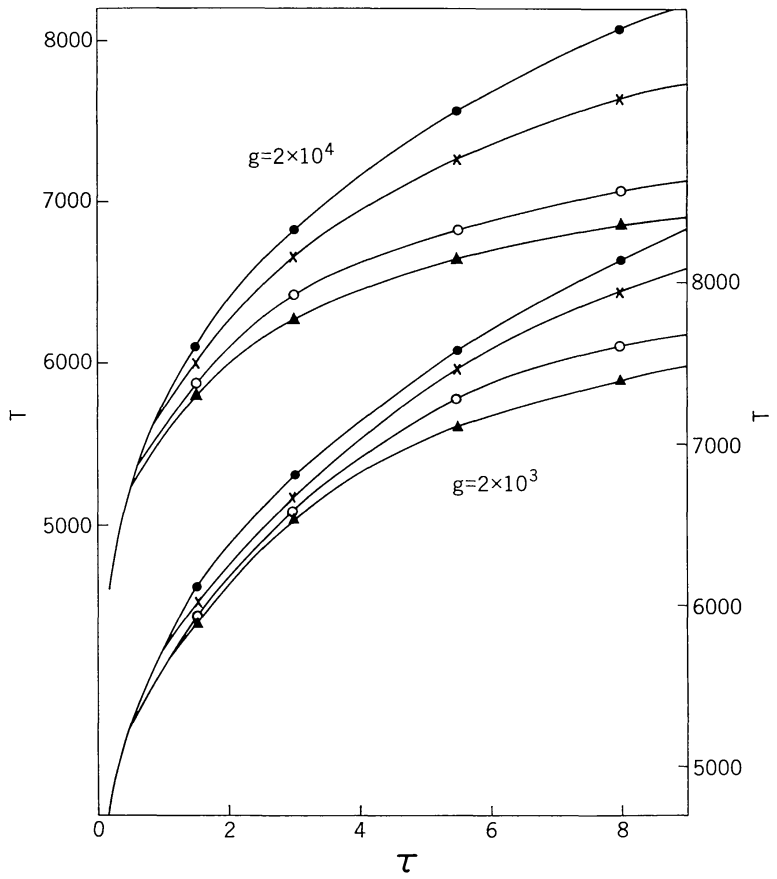

Fig. 9. Temperature distribution is plotted as a function of τ for $T_e = 5000$ K. Curves with dots, crosses, circles and triangles refer to hydrogen-to-metal ratios of 1, 5, 40 and 100 times the solar value.

ties of the star (KRISHNA SWAMY, 1966a, 1967, 1968a, b, c; COHEN and STROM, 1968; DENNIS, 1968). In fact, the reason for the lower effective temperatures obtained by previous investigators (MELBOURNE, 1960; STROM *et al.*, 1967) in the study of metal-deficient stars seems to be the result of the use of purely radiative models.

One also finds from Figure 1 that for late-type stars convection starts at $\tau \gtrsim 0.1$. Based on the above discussion of metal-deficient stars, we also expect convection to play an important role in the discussion of late-type stars. Recently, AUMAN (1968) has calculated accurate model atmospheres of late-type stars and has discussed the problem of convection in these stars.

References

AUMAN, J.: 1968 (Preprint).
BÖHM, K.-H.: 1963, *Astrophys. J.* **137,** 881.
BÖHM-VITENSE, E.: 1958, *Z. Astrophys.* **46,** 108.
CAYREL, R. and JUGAKU, J.: 1963, *Ann. Astrophys.* **26,** 495.
COHEN, J. G. and STROM, S. E.: 1968, *Astrophys. J.* **151,** 623.
DENNIS, T. R.: 1968, *Astrophys. J. Letters* **151,** L47.
FISCHEL, D.: 1968, *Astrophys. J.* **152,** 353.

GOLDBERG, L., MULLER, E. A., and ALLER, L. H.: 1960, *Astrophys. J. Suppl. Ser.* **5,** 1.
KRISHNA SWAMY, K. S.: 1961, *Astrophys. J.* **134,** 1017.
KRISHNA SWAMY, K. S.: 1966a, *Astrophys. J.* **145,** 174.
KRISHNA SWAMY, K. S.: 1966b, *Astrophys. J.* **146,** 731.
KRISHNA SWAMY, K. S.: 1967, *Astrophys. J.* **150,** 1161.
KRISHNA SWAMY, K. S.: 1968a, *Astrophys. J.* **152,** 477.
KRISHNA SWAMY, K. S.: 1968b, in *Symposium on Low Luminosity Stars*, Charlottesville (in press).
KRISHNA SWAMY, K. S.: 1968c (in preparation).
MELBOURNE, W. G.: 1960, *Astrophys. J.* **132,** 101.
MITCHELL, W. E.: 1959, *Astrophys. J.* **129,** 369.
SCHWARZSCHILD, K.: 1906, *Gött. Nachr.*, No. 1, p. 41.
STROM, S. E., COHEN, J. G., and STROM, K. M.: 1967, *Astrophys. J.* **147,** 1038.
UNDERHILL, A. B.: 1949, *Monthly Notices Roy. Astron. Soc.* **109,** 562.
UNSÖLD, A.: 1930, *Z. Astrophys.* **1,** 138.
UNSÖLD, A.: 1938, *Physik der Sternatmosphären*, Springer, Berlin, p. 382.
VARDYA, M. S.: 1965, *Monthly Notices Roy. Astron. Soc.* **129,** 205.
VARDYA, M. S.: 1966, *Monthly Notices Roy. Astron. Soc.* **134,** 347.